The Journal of Neuroscience, April 1995, 15(4): 2720–2732

$GABA_A$/Benzodiazepine Receptors in Acutely Isolated Hippocampal Astrocytes

Douglas D. Fraser,[1] Steven Duffy,[1] Kimon J. Angelides,[2] Jose L. Perez-Velazquez,[3] Helmut Kettenmann,[4] and Brian A. MacVicar[1]

[1]Neuroscience Research Group, University of Calgary, Calgary, Alberta, Canada T2N 4N1, [2]Department of Cell Biology, Baylor College of Medicine, Houston, Texas, [3]Playfair Neuroscience Unit, Toronto Western Hospital, Toronto, Ontario, Canada, and [4]Max-Delbrüak Center for Molecular Medicine, Berlin-Buch, Germany

The properties of GABA receptor–mediated responses were examined in noncultured astrocytes, acutely isolated from the mature rat hippocampus. Whole-cell patch clamping revealed a GABA-activated Cl^- conductance that was mimicked by the $GABA_A$ receptor agonist muscimol and depressed by the $GABA_A$ antagonists bicuculline and picrotoxin. The $GABA_A$-activated currents were potentiated by the barbiturate pentobarbital and the benzodiazepine diazepam. The benzodiazepine inverse agonist DMCM either enhanced or depressed the astrocytic $GABA_A$-mediated responses, suggesting receptor heterogeneity with respect to pharmacologic profiles. In addition, GABA evoked an increase in $[Ca^{2+}]_i$, measured by indo-1 fluorometry, which was depressed in the presence of verapamil or picrotoxin. A $GABA_A$-induced depolarization, therefore, causes Ca^{2+} influx through voltage-gated Ca^{2+} channels. The expression and subcellular localization of $GABA_A$ receptors and its subunits were examined using immunohistochemical and fluorescent benzodiazepine binding techniques. Polyclonal antisera raised against the $GABA_A$/benzodiazepine receptor, which recognizes multiple subunit isoforms, labeled receptors on the astrocytic cell body and most large processes. In contrast, antisera generated against either α_1 or β_1 subunit peptides revealed immunoreactivity predominantly on a subset of processes. To determine the subcellular distribution of membrane-bound receptors, a fluorescent benzodiazepine derivative was superfused over live astrocytes and visualized with laser-scanning confocal microscopy. Specific fluorescence was distributed in discrete clusters on the cell soma and a subset of distal processes. Collectively, these data support the view that astrocytes, like neurons, express $GABA_A$ receptors and target subunit isoforms to distinct cellular localizations. Astrocytic $GABA_A$ receptors may be involved in both $[Cl^-]_o$ and $[pH]_o$ homeostasis, and a GABA-evoked increase in $[Ca^{2+}]_i$ could serve as a signal between GABAergic neurons and astrocytes.

[Key words: astrocyte, GABA receptor, Cl^- current, benzodiazepines, barbiturates, voltage-activated Ca^{2+} influx, Western blot, immunocytochemistry, ligand binding]

Electrophysiological studies indicate that cultured astrocytes and oligodendrocytes express receptors for GABA (reviewed by Blankenfeld and Kettenmann, 1992; Fraser et al., 1994). The astrocytic $GABA_A$ receptor shares many pharmacological properties with the neuronal receptor, including modulation by barbiturates, benzodiazepines, and steroids. $GABA_A$ receptor–mediated responses have also been recorded from astrocytes in hippocampal (MacVicar et al., 1989; Steinhäuser et al., 1993, 1994) and retinal (Clark and Mobbs, 1992) slices, oligodendrocytes in corpus callosum slices (Berger et al., 1992), Bergmann glia in cerebellar slices (Müller et al., 1994), and stellate glia in the intact pituitary pars intermedia (Mudrick-Donnon et al., 1993). Although the functional aspects of $GABA_A$ receptor activation on astrocytes is not known, further investigations of the physiologic, pharmacologic, and anatomic properties of these receptors may lead to a more clear understanding of their function in the CNS.

Recently, a procedure for acute isolation of astrocytes from mature tissue was described (MacVicar et al., 1992; Tse et al., 1992). By using this preparation, not only is the possibility of culture artifact avoided, but agonists can be applied rapidly and uniformly, which is not possible in whole tissue. For example, saturating concentrations of GABA were required to activate glia receptors embedded in tissue slices and, thus, the dose–response relation and allosteric modulation could not be determined accurately (e.g., Berger et al., 1992; Steinhäuser et al., 1993, 1994). The first objective of this study was, therefore, to confirm the presence of $GABA_A$ receptors on acutely isolated astrocytes and to investigate the electrophysiologic and pharmacologic properties of these receptors using whole-cell patch clamp and rapid perfusion techniques.

In most neurons, activation of $GABA_A$ receptors causes an influx of Cl^- and a membrane hyperpolarization (Alvarez-Leefmans and Russels, 1990). In contrast, activation of glial $GABA_A$ receptors, in both oligodendrocytes and astrocytes, always leads to an efflux of Cl^- (Hoppe and Kettenmann, 1989; MacVicar et al., 1989). In glia, the nonpassive distribution of Cl^- is based on the activity of two inwardly directed Cl^- transporters: an $Na^+/K^+/2Cl^-$ cotransporter and a Cl^-/HCO^-_3 exchanger (Kettenmann, 1990; Kimelberg, 1990). Studies have shown that the

Received Apr. 13, 1994; revised Aug. 25, 1994; accepted Sept. 7, 1994.

We are grateful to the laboratory of Dr. Samuel Weiss for assistance with immunocytochemistry, Dr. H. Sontheimer for a manuscript preprint, and Dr. L. A. Mudrick-Donnon for critical comments on the manuscript. This work was supported by a grant from the Medical Research Council (MRC) of Canada. D.D.F. is a recipient of studentships from the MRC (Canada), Alberta Heritage Foundation for Medical Research (AHFMR), and Savoy Foundation for Epilepsy Research. S.D. held an AHFMR studentship. B.A.M. is an AHFMR Scientist and The Ciba Geigy chair for schizophrenia research.

Correspondence should be addressed to Brian A. MacVicar at the above address.

Copyright © 1995 Society for Neuroscience 0270-6474/95/152720-13$05.00/0

Cl^- equilibrium potential in astrocytes can be as positive as −35 mV, leading to a membrane depolarization of ~40 mV following $GABA_A$ receptor activation (Kettenmann and Schachner, 1985). A $GABA_A$-induced membrane depolarization of this magnitude would surpass the activation threshold for voltage-gated Ca^{2+} channels which have been identified in cultured (MacVicar, 1984; MacVicar and Tse, 1988; Barres et al., 1989) and acutely isolated (Duffy and MacVicar, 1994) astrocytes. It is not known, however, whether $GABA_A$-induced membrane depolarizations cause a change in $[Ca^{2+}]_i$. It is possible that a $GABA_A$-induced increase in $[Ca^{2+}]_i$, which has been reported recently for cultured glial precursor cells (Kirchhoff and Kettenmann, 1992), could result in activity-dependent modification of astrocytic signaling pathways. The second objective of this study was, therefore, to measure $[Ca^{2+}]_i$ with indo-1 fluorometry to determine whether $GABA_A$-induced membrane depolarization evokes Ca^{2+} influx through voltage-gated Ca^{2+} channels.

Knowledge of the subcellular distribution of $GABA_A$ receptors within single astrocytes is important for determining the functional aspects of receptor expression. For example, $GABA_A$ receptors may be targeted and expressed on astrocytic processes, which are in close association with synaptic regions (Peters et al., 1991). Molecular cloning and low-stringency screening of cDNA libraries have identified at least 15 $GABA_A$ receptor subunits separated by degree of homology into five families (α_{1-6}, β_{1-4}, γ_{1-3}, δ, ρ; reviewed by Olsen and Tobin, 1990; Burt and Kamatchi, 1991). Recombinant studies revealed further that subunit combinations differ in sensitivity from agonists and allosteric modulation. In astrocytes, sequence- and subunit-specific antibodies could reveal the expression of particular subunits and their isoforms which join to construct functional $GABA_A$ receptors. The third objective of this study was, therefore, to determine the expression and subcellular distribution of $GABA_A$/benzodiazepine receptors and their subunits using polyclonal antibodies and a novel fluorescent benzodiazepine derivative.

The results demonstrate that $GABA_A$ receptors with unique pharmacologic profiles are expressed in mature astrocytes, that $GABA_A$ receptor activation depolarizes astrocytes sufficiently to open voltage-gated Ca^{2+} channels, and that $GABA_A$ receptors and subunits are targeted to distinct cellular locations.

This work has been presented in abstract form (Fraser et al., 1992, 1993).

Materials and Methods

Acute isolation of hippocampal astrocytes. The isolation technique for hippocampal astrocytes has been described previously (MacVicar et al., 1992; Tse et al., 1992). Briefly, transverse hippocampal slices (500 μm) were obtained from Sprague–Dawley rats (2–6 weeks postnatal) and placed in artificial cerebrospinal fluid (aCSF) containing (in mM) 124 NaCl, 5 KCl, 1.3 $MgCl_2$, 2 $CaCl_2$, 26 $NaHCO_3^-$, and 10 D-glucose (pH 7.35; 280 mOsm). Slices were transferred to a magnetic stirring flask filled with 30 ml of aCSF containing papain (24–28 U/ml; Sigma, P-4762), the papain activator L-cysteine (1 mg/100 U papain; Sigma, C-1276), and 1 mM kynurenic acid (Sigma, K-3375). During enzymatic digestion, the solution was stirred continuously and aerated with 95% O_2/5% CO_2. Following the 1 hr enzymatic treatment, the slices were washed several times with fresh aCSF and stored at room temperature in aCSF. When needed, the CA1 region was dissected free and mechanically triturated with fire-polished Pasteur pipettes in HEPES-buffered DMEM which contained 0.1 mM leupeptin (Sigma, L-2884) and 1 mM kynurenic acid. Isolated cells in suspension were allowed to either settle onto poly-L-lysine-coated coverslips for 20 min or bind securely to poly-L-lysine-coated coverslips by brief centrifugation before the onset of constant superfusion with selected external solutions.

Electrophysiological recording. Patch electrodes were pulled from 1.5 mm o.d. thin-walled glass (TW 150F-4, World Precision Instruments) on a Flaming-Brown micropipette puller (P-87, Sutter Instrument Company). Electrodes had a tip resistance of 4–8 MΩ when tested in the external solution. The various K^+ conductances of the cell membrane (Tse et al., 1992) were suppressed by using an intracellular solution containing (in mM) 130 CsCl, 4 $MgCl_2$, 1 $CaCl_2$, 10 HEPES, 10 EGTA, and 2 Mg^{2+}-ATP (pH 7.2) in combination with an extracellular solution containing (in mM) 119 NaCl, 3 CsCl, 2 $MgCl_2$, 2 $CaCl_2$, 5 $BaCl_2$, 10 D-glucose, and 10 HEPES (pH 7.35). Intracellular Ca^{2+} concentration was calculated to be ~11 nM. In some experiments, NaCl was substituted with equimolar Na^+-gluconate to shift the Cl^- equilibrium potential. Current recordings were obtained using a single electrode amplifier (Axopatch-1A) in voltage-clamp mode, and filtered (four-pole Bessel) at a low-pass bandwidth of 200 Hz (−3 dB). Analog current waveforms were displayed and digitized simultaneously by PCLAMP software via a Tl-125 A/D interface (Axon Instruments). Liquid junction potentials between electrode and bath solutions were measured and compensated subsequently. All recordings were performed at room temperature (~21°C) and data is reported as the mean ± standard error.

Drug application. Drugs were applied to single cells in the extracellular solution described above by a rapid perfusion system consisting of multiple stainless steel inlet pipes (i.d. 0.43 mm) secured in a triangular-shaped plexiglass head with one common outlet pipe (i.d. 0.33 mm). The plexiglass head was mounted on a hydraulic manipulator via a 10 cm shaft and positioned within 0.5–1.0 mm of the cell to insure a uniform flow of solution across the entire membrane. Control and drug-containing solutions were gravity fed from multiple reservoirs (60 ml syringes) through consecutively smaller polyethylene tubing (from i.d. 1.14 mm to i.d. 0.58 mm) to the inlet pipes. The tubing containing control solution was split by a "normally open" solenoid valve (Lee Co., LFYAO518232H), whereas tubing containing drugs was split by "normally closed" solenoid valves (Lee Co., LFVX0500250A). The cell was bathed continuously by a rapidly flowing stream of control solution between drug applications. Rapid solution changes were achieved by simultaneously closing the control valve and opening a drug valve. Each valve was controlled by a solenoid driver coupled to a TTL-pulse from the A/D interface.

Fluorometric measurement of intracellular Ca^{2+}. Intracellular Ca^{2+} ($[Ca^{2+}]_i$) changes were monitored by measuring indo-1 fluorescence. Astrocytes were loaded with dye by adding 50 μg indo-1/AM (Molecular Probes, I-1203; sonicated with 10 μl DMSO and 10% pluronic acid) to the trituration media. The period during which the cells were initially dissociated and allowed to settle was sufficient for dye loading. Once adhered to the cover slip, astrocytes were superfused with aCSF. Single astrocytes were illuminated at 380 nm and the fluorescence outputs at 405 and 485 nm were measured simultaneously using a dichroic mirror and two photomultiplier tubes (PMT; Hamamatsu, C1053-01). Illumination frequency (1–2 Hz) and duration (50 msec) were controlled by an electronic shutter (UniBlitz). PMT current output was converted to voltage and digitized at 200 Hz using a Tl-125 A/D interface and AXOTAPE software (Axon Instruments). Following each experiment, autofluorescence was determined by superfusion of 1 mM Mn^{2+} in the presence of the nonfluorescent Ca^{2+} ionophore 4-bromo A-23187 (1 μM; Molecular Probes, B-1494). Intracellular Ca^{2+} concentration was estimated by the equation from Grynkiewicz et al. (1985):

$$[Ca^{2+}]_i = K_d\ [(R - R_{min})/(R_{max} - R)]\ [S_f/S_b],$$

where K_d is 250 nm, R_{min} is 0.2, R_{max} is 3.0, and S_f/S_b was 10.667. All values except for K_d were determined experimentally on our recording setup using calibrated Ca^{2+} solutions. Drugs were applied by changing the superfusion in the bath. The perfusion rate was approximately 1.0 ml/min, which allowed a complete solution change in the bath (volume 150 μl) in <30 sec.

Antibody production. A polyclonal antibody which recognizes the $GABA_A$/benzodiazepine receptor complex was generated against the affinity-purified $GABA_A$ receptor. Purification of the protein was carried out on a benzodiazepine affinity column according to Sigel et al. (1982). One hundred to three hundred micrograms of the purified receptor was injected into the lymph nodes of New Zealand White rabbits.

Subunit-specific antibodies were generated in New Zealand White rabbits immunized with peptides corresponding to the N and C termini of the α_1 and β_1 subunits. The following subunit-specific sequences were α_1 N-terminus, Q-P-S-L-Q-D-E-L-K-D-N-T-T-V-F-C; α_1 C-terminus, C-L-N-R-E-P-Q-L-K-A-P-T-P-H-Q; β_1 N-terminus, H-S-A-N-E-P-S-N-M-S-Y-V-K-E-T-V-C; β_1 C-terminus, L-F-N-V-V-Y-W-L-Y-V-H-C. Peptides were coupled to rabbit serum albumin (RSA) with

glutaraldehyde (Chow et al., 1984) and by reacting the C-terminal cysteine residue with succinimidyl-phenyl-maleimide (Gitman et al., 1985). Rabbits were injected at multiple intradermal sites with 1 mg of the conjugated peptide in the RIBI adjuvant system (RIBI Immunochem., Hamilton, MN).

For all antibodies, booster injections were performed every 2–3 weeks. The animals were exsanguinated after 10 weeks of the initial immunization. Immunoglobulin fractions (IgG) were precipitated in saturated ammonium sulfate, dialyzed against phosphate buffer, and stored at −20°C. IgG fractions were assayed for recognition of the $GABA_A$ receptor by dot blots and Western blotting of affinity-purified $GABA_A$/benzodiazepine receptors and crude glycoproteins from rat brain.

Western blot analysis. Purified $GABA_A$ receptors or crude glycoproteins were electrophoresed on 4–15% or 7.5% linear gradient polyacrylamide SDS gels, respectively, according to the method of Laemmli (1970). Gels were silver stained or electrophoretically transferred to nitrocellulose by the method of Towbin et al. (1979). Nitrocellulose membranes containing the transferred proteins were blocked with 5% nonfat dry milk in TBST [10 mM Tris-HCl, pH 8.0, 0.15 M NaCl, 0.02% Tween-20 (Sigma, P-1379)] and incubated with several dilutions of the antibodies in the same buffer at 4°C overnight. Blots were then washed three times with fresh TBST and incubated with alkaline phosphatase conjugated to goat-anti-rabbit IgG (Promega) for 2 hr at room temperature. The blots were washed twice in TBST, rinsed with water, and developed with *p*-nitrotetrazolium blue chloride (0.1 mg/ml; Sigma) and 5-bromo-4-chloro-3-indolyl phosphate p-toluidine salt (0.005 mg/ml; Pierce).

Glycoprotein fractions used for immunoblotting were obtained from rat brain by chromatography on a wheat germ agglutinin Sepharose-4B column (WGA-Sepharose-4B). Briefly, rat brain was homogenized in 10 mM Tris-HCl (pH 7.4) with 300 mM sucrose. This homogenate was centrifuged at 1000 × *g* for 12 min, and the supernatant centrifuged again at 27,000 × *g* for 35 min. The pellet obtained was resuspended and homogenized in the same buffer without sucrose, and centrifuged as before. The final pellet was homogenized in 10 mM Tris-HCl (pH 7.4), 2.5% Triton X-100, and 150 mM KCl, shaken for 30 min, and centrifuged at 100,000 × *g* for 60 min. The supernatant obtained contained the solubilized proteins that were applied to a WGA-Sepharose 4B chromatography column. Glycoproteins were eluted from the column with 25 mM *N*-acetylglucosamine. Fractions were assayed by ^{3}H-flunitrazepam binding to determine fractions that contained the $GABA_A$/benzodiazepine receptor. Nonspecific binding was measured in the presence of 300 nM clonazepam. ^{3}H radioactivity was counted in Scintiverse on a Beckman LS-1801 Scintillation Counter. In all steps, a cocktail of protease inhibitors (Sigma) was used, which contained iodoacetamide (1 mM), *o*-phenanthroline (1 mM), leupeptin (1 mM), aprotinin (1 mM), and pepstatin (0.5 mg/ml).

Immunocytochemistry. Isolated cells, adhered securely to coverslips, were fixed with 4% paraformaldehyde in phosphate-buffered saline (PBS) for 10 min at room temperature. Membranes were permeabilized with 95% EtOH/5% acetic acid for 10 min at −10°C. A mouse monoclonal antibody directed against glial fibrillary acidic protein (MAb-GFAP, 1:100; Boehringer Mannheim) and one of the rabbit polyclonal antibodies generated against the $GABA_A$/benzodiazepine receptor (PAb-967, 1:100–250), an α_1 subunit peptide (PAb-B, 1:100), or a β_1 subunit peptide (PAb-Q, 1:100) were applied together in PBS containing 10% normal goat serum, 3% bovine serum albumin, and 0.05% Tween-20 for 2 hr at 37°C. Antigen/antibody complexes were visualized by incubation of coverslips in fluorescein-conjugated goat antibody to mouse IgG (1:100; Jackson) and rhodamine-conjugated goat antibody to rabbit IgG (1:100; Jackson). All steps were separated by five 10 min washes in PBS containing 0.05% Tween-20. Coverslips were then mounted with Fluorosave (Calbiochem Inc.) on glass slides and viewed with a Nikon microscope equipped with appropriate filter sets. Images were scanned in RGB (1000 dpi; Leafscan 35) from Kodachrome color film, converted to a black/white scale, and final output produced by a Linotronic printer. Controls at the immunohistochemical level included omission of primary antibodies or replacement of polyclonal antibodies with preimmune sera.

Fluorometric mapping of GABA/benzodiazepine receptors. A fluorescent benzodiazepine derivative was prepared by alkylation of the amide on Ro 7-1986 by BODIPY alkyl halide. This compound maintains high affinity and specificity for central benzodiazepine receptors and has been characterized previously by mass spectrometry, equilibrium binding to brain membranes, and fluorescence microscopy (Velazquez et al., 1989; McCabe et al., 1990). Astrocytes, adhered securely to coverslips, were placed in the perfusion chamber on an upright laser-scanning confocal microscope (Meridian Instr., Inc.). Once an astrocyte had been identified visually by its distinct morphology, the chamber was perfused with 5 nM of the BODIPY-Ro 7-1986 derivative in phosphate-buffered saline (PBS) for 20 min. Total binding was determined following a 2 min wash with PBS. Nonspecific binding was determined as above, with the exception that the derivative was coperfused with 500 nM diazepam. All binding experiments were performed at reduced temperatures (<8°C) to suppress endocytosis of the derivative. Fluorescent images from cells were obtained with a silicon-intensified target camera (SIT; Hamamatsu, C2400) through a 40×, 0.75 numerical aperture, water-immersion objective (Zeiss). Video frames were averaged and digitized into a 512 × 480 pixel array by an eight-bit A/D board of an image processor (Series 151; Imaging Technology Inc.) controlled by a personal computer (Packard-Bell 386). Digital images were enhanced by thresholding and histogram stretching; pixel intensities were determined by averaging. At the completion of the binding experiments, a subset of cells was fixed and stained for GFAP to verify its astrocytic phenotype.

Results

Identification and characteristics of astrocytes

Acutely isolated astrocytes from the hippocampal CA1 region are known to be immunoreactive for GFAP (MacVicar et al., 1992; Tse et al., 1992), the predominant protein of intermediate filaments in astroglia. They were identified visually by distinct morphological features, including a small soma diameter (~8 μm) and bushy processes with random orientation. In contrast, pyramidal neurons and interneurons were easily recognized by their larger smooth cell bodies and 1–3 tapering dendrites (e.g., Kay and Wong, 1986; Fraser and MacVicar, 1991). Neurons isolated simultaneously do not stain for GFAP (Tse et al., 1992). Identification of cell type can also be inferred by membrane current patterns evoked by voltage steps or capacitance measurements obtained via a calibrated potentiometer. In astrocytes, inward Na^+ currents were not observed under whole-cell voltage clamp (Fig. 1) and action potentials could not be generated in the current-clamp mode (data not shown). In contrast, neurons coisolated with astrocytes exhibited robust inward transient and sustained currents carried by Na^+ and Ca^{2+}/Ba^{2+}, respectively (Fig. 1). Typically, the larger astrocytic surface area was reflected by large capacitance values (61 ± 3 pF, range 25–100 pF, n = 65/77; 12 cells could not be estimated because of values >100 pF), whereas neurons had smaller values (12 ± 1 pF, range 4–21 pF, n = 32).

GABA-activated membrane currents

In all pyramidal neurons (n = 32) and 91% of astrocytes (n = 77/85), application of GABA activated an inward current when the membrane potential was voltage clamped at −80 mV (Fig. 1). At a GABA concentration of 50 μM, the peak inward current amplitude in pyramidal neurons and astrocytes was 1562 ± 146 pA (range 791–2500 pA, n = 14) and 486 ± 38 pA (range 38–2000 pA, n = 50), respectively. In both cell types, the current activated quickly, followed by marked desensitization.

The peak amplitudes of both neuronal and astrocytic GABA-activated currents were concentration dependent. To reveal the dose–response relation for both cell types, variable concentrations of GABA (1, 3, 10, 30, 100, 300, 1000 μM) were applied for 3 sec at 5 min intervals (Fig. 2). This delay was sufficient for full recovery from desensitization. The peak amplitude of GABA responses was plotted as a function of GABA concentration, normalized to a saturating response elicited by 1 mM GABA. The peak current amplitude evoked by 1 mM GABA was 2078 ± 349 pA for pyramidal neurons (range 679–4000

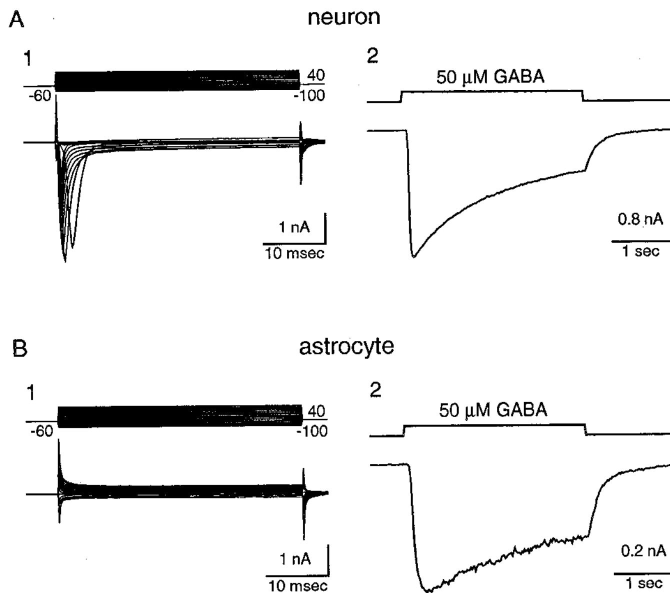

Figure 1. Membrane current patterns and GABA-activated inward currents in acutely isolated CA1 pyramidal neurons and astrocytes as revealed by whole-cell patch clamp. *A1,* A pyramidal neuron was identified by its characteristic morphology and typical neuronal current pattern when voltage clamped to hyper- and depolarizing membrane potentials (see Materials and Methods for description of solutions). Depolarization revealed a large amplitude transient inward current and a smaller sustained inward current. The whole-cell capacitance was 16 pF. *A2,* Rapid application of 50 μM GABA to the neuron in *A1* evoked an inward current of 2000 pA when voltage clamped at −80 mV. *B1,* An acutely isolated astrocyte was identified by its characteristic morphology and passive membrane response when voltage clamped to hyper- and depolarizing membrane potentials (see Materials and Methods for description of solutions). The whole-cell capacitance was 63 pF. *B2,* Rapid application of 50 μM GABA to the astrocyte in *B1* evoked an inward current of 500 pA when voltage clamped at −80 mV.

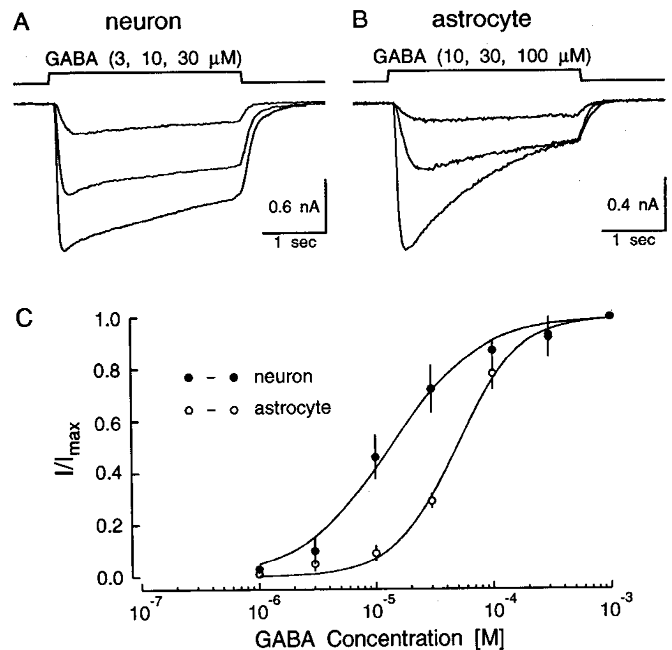

Figure 2. Dose–response relation of neuronal and astrocytic GABA-activated inward currents. *A,* Rapid application of 3, 10, or 30 μM GABA to a CA1 pyramidal neuron revealed inward currents of increasing amplitude from a holding potential of −80 mV. These concentrations represent the linear portion of the concentration–response curve. The whole-cell capacitance was 5 pF. *B,* Rapid application of 10, 30, or 100 μM GABA to an astrocyte revealed inward currents of increasing amplitude from a holding potential of −80 mV. These concentrations represent the linear portion of the concentration–response curve. The whole-cell capacitance was 52 pF. *C,* The dose–response relation for the neuronal and astrocytic GABA-evoked inward current, in which the peak current at variable concentrations was normalized to the maximal response obtained with 1 mM GABA. Each point represents the mean ± SEM from three cells.

pA, n = 9) and 1064 ± 167 pA for astrocytes (range 275–2050 pA, n = 12). Responses significantly above the noise level could be elicited with 1–3 μM GABA and the current amplitude increased in a sigmoidal fashion with the GABA concentration (Fig. 2*C*). The dose–response relations were in agreement with the conventional expression

$$I/I_{max} = 1/(1 + (EC_{50}/[GABA])^n,$$

where I is the amplitude of the GABA-activated current, EC_{50} is the GABA concentration which evokes the half-maximal response, and n is the Hill coefficient. The EC_{50} and hill coefficient values for neurons were 14 μM and 1.1, whereas astrocytes had values of 50 μM and 1.6. The maximal current amplitudes and EC_{50} values suggested that GABA acting at neuronal receptors had greater potency and efficacy. The hill coefficient values suggested that the astrocytic receptors must bind a minimum of two GABA molecules to open the receptor/ionophore, whereas the receptors on pyramidal neurons have only one binding site or slight allosteric interaction between two putative sites (Bormann and Clapham, 1985).

Reversal potential of the GABA-activated current

The ionic species permeating the astrocytic GABA receptor/ionophore was identified by analyzing the reversal potential of the GABA-induced current (Fig. 3). Two strategies were employed to vary the membrane potential. First, the membrane potential was altered to steady-state levels of −80, −60, −40, −20, 0, 20, 40, and 60 mV for several seconds followed by a rapid application of GABA (Fig. 3*A*; n = 4). The current induced by 50 μM GABA reversed in polarity close to 0 mV. Second, the membrane potential was ramped from −100 to 100 mV over 4 sec (Fig. 3*B*). To resolve the GABA-activated current, the ramp-induced current in standard bathing solution was subtracted from that obtained in the presence of 50 μM GABA (Fig. 3*C*). The GABA current reversed at 1.0 ± 1.8 mV (range −3–7 mV, n = 5). These values coincided with the expected Cl^- equilibrium potential (E_{Cl} = 0 mV) as derived by the Nernst equation. Moreover, decreasing the $[Cl^-]_o$ concentration to 90 and 55 mM, by substitution with the nonpermeable anion gluconate, shifted the reversal potential to 12.6 ± 0.8 (range 11–14 mV, n = 3) and 22.3 ± 1.5 (range 20–25 mV; n = 3) mV, respectively (Fig. 3*D*). These values are in close agreement with the calculated Cl^- equilibrium potentials of 11 and 24 mV. These data indicate that GABA activates a Cl^- conductance in acutely isolated astrocytes, indicating the expression of $GABA_A$ receptors.

Pharmacological properties of the GABA response

The GABA-activated current recorded from acutely isolated astrocytes was characterized further by testing drugs affecting $GABA_A$-mediated responses as described in other cells. To ensure a stable response, several GABA-activated currents were monitored before and after application of a particular drug. Consec-

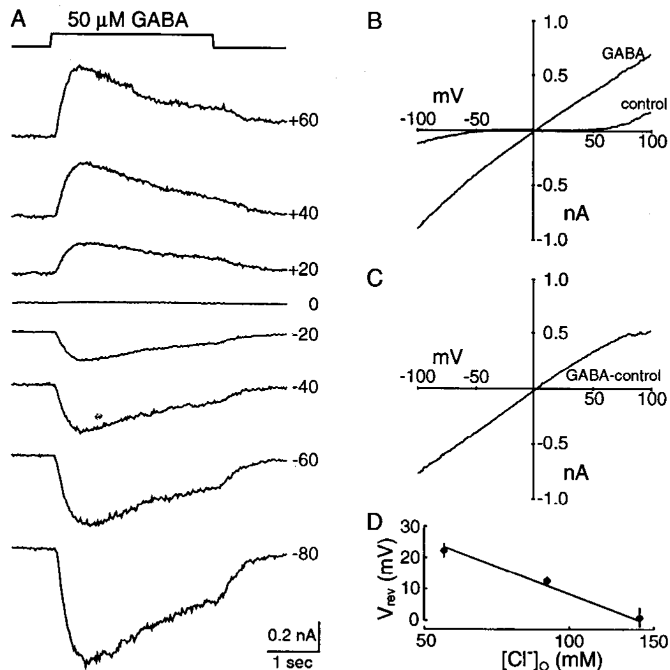

Figure 3. The reversal potential of the GABA-activated inward current in astrocytes corresponds to the equilibrium potential of Cl^- (E_{Cl} = 0 mV). *A*, GABA-activated currents at variable membrane potentials as indicated. The current reversed in polarity close to 0 mV. The whole-cell capacitance was 64 pF. *B*, A computer-generated ramp paradigm changed the membrane potential from −100 to 100 mV in control and in the presence of 50 μM GABA. Note the incompletely blocked inward and outward rectification characteristic of astrocytes. *C*, The GABA-activated current was obtained by subtracting the curve obtained in control from the curve obtained in the presence of GABA. The current reverses close to 0 mV. The whole-cell capacitance was 100 pF. *D*, The reversal potential for the GABA-activated current, obtained as described in *B* and *C*, for different extracellular Cl^- concentrations. The *straight line* represents the Cl^- equilibrium potential as calculated by the Nernst equation. Each point represents the mean ± SEM from 3–5 cells.

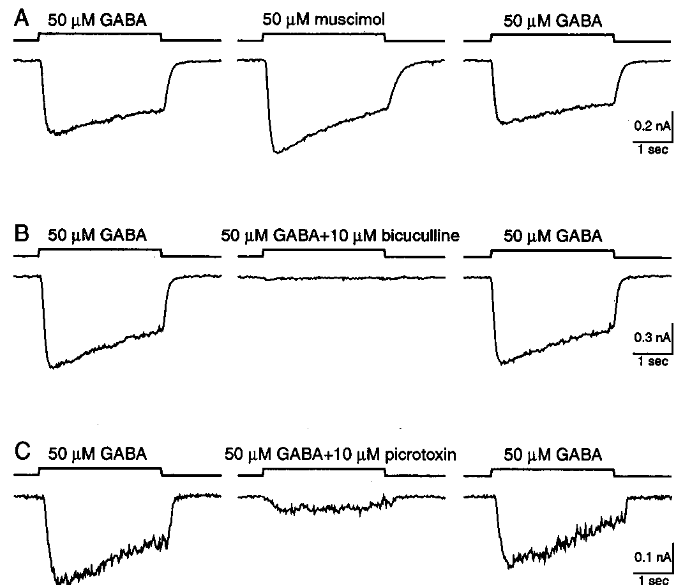

Figure 4. Pharmacological characteristics of the astrocytic GABA current suggest a $GABA_A$ receptor. *A*, Rapid application of 50 μM GABA evoked control currents that were similar to those evoked by 50 μM muscimol, a specific $GABA_A$ receptor agonist. The inward current evoked by an equivalent concentration of muscimol, however, was typically larger in amplitude. The whole-cell capacitance was 100 pF. *B*, Inward currents were evoked by rapid application of 50 μM GABA and could be reversibly depressed by coapplication the $GABA_A$ receptor antagonist bicuculline (10 μM). The whole-cell capacitance was 98 pF. *C*, Inward currents were evoked by rapid application of 50 μM GABA and could be reversibly depressed by coapplication the Cl^- channel blocker picrotoxin (10 μM). The whole-cell capacitance was 55 pF.

utive tests were separated by 5 min. The $GABA_A$ receptor agonist muscimol (50 μM) mimicked the GABA-induced response (Fig. 4*A*). The amplitude of the muscimol response, however, was enhanced with respect to GABA by 45 ± 15% (range 6–93%, n = 5). Coapplication of GABA and 10 μM of the $GABA_A$ receptor antagonist bicuculline or 10 μM of the Cl^- channel blocker picrotoxin depressed the GABA responses by 79 ± 15% (range 48–96%, n = 3) or 74 ± 11% (range 52–86%, n = 3), respectively (Fig. 4*B*,*C*). Depression of the GABA-induced current was reversible upon washout of the antagonists. This set of experiments indicates that the GABA-induced inward current is caused by the activation of $GABA_A$ receptors.

The pharmacological properties of the astrocytic $GABA_A$ receptor were characterized by testing the effect of $GABA_A$ receptor modulators, namely the barbiturate pentobarbital, the benzodiazepine diazepam and the benzodiazepine inverse agonist DMCM. Similar to neurons, sodium pentobarbital (25 μM; Fig. 5*A*) and diazepam (10 μM; Fig. 5*B*) potently and reversibly enhanced the astrocytic GABA-activated current by 159 ± 51% (range 42–315%, n = 5) and 56 ± 14% (range 18–260%, n = 17), respectively. Surprisingly, DMCM either potentiated (15 ± 4%, range 7–25%, n = 3/15; Fig. 5*C*) or depressed (19 ± 3%, range 8–40%, n = 12/15; Fig. 5*D*) the astrocytic GABA-activated current, indicating heterogeneity with respect to receptor expression. In contrast, GABA-activated currents recorded in pyramidal neurons were depressed consistently by coapplication of DMCM (44 ± 5%, range 33–56%, n = 7; Fig. 5*E*). These experiments suggest that astrocytic GABA receptors share similarities with, but are not identical to, neuronal $GABA_A$ receptors.

GABA-induced Ca^{2+} responses

GABA-induced changes of intracellular Ca^{2+} were analyzed in acutely isolated astrocytes using the AM form of indo-1 and standard fluorometric techniques. Bath superfusion of GABA (1 mM) caused a transient increase in $[Ca^{2+}]_i$ in 30% of the astrocytes tested (n = 11/33; Fig. 6). At rest, the ratio (R) of the fluorescence intensities at two wavelengths (405 nm/485 nm) was 0.37 ± 0.04 (n = 11). Application of GABA increased the ratio to 0.41 ± 0.5 (n = 11). These values corresponded to an average increase in $[Ca^{2+}]_i$ from 172 nM in control to 296 nM in the presence of GABA. Increasing external K^+ from control levels of 5 mM to 50 mM also increased $[Ca^{2+}]_i$ by opening verapamil-sensitive voltage-activated Ca^{2+} channels (Fig. 6*A*; Duffy and MacVicar, 1994). To investigate the possibility that GABA also increased $[Ca^{2+}]_i$ by influx through voltage-activated Ca^{2+} channels secondary to a $GABA_A$-induced membrane depolarization, the sensitivity of GABA-evoked $[Ca^{2+}]_i$ changes to verapamil and picrotoxin was examined. The Ca^{2+} channel blocker verapamil (150 μM) reversibly depressed the GABA-induced increase in $[Ca^{2+}]_i$ (n = 2; Fig. 6*B*). Verapamil did not have an inhibitory effect, however, on the magnitude of the whole-cell GABA-activated current (data not shown; n = 5). Picrotoxin (100 μM), which specifically blocks Cl^- channels,

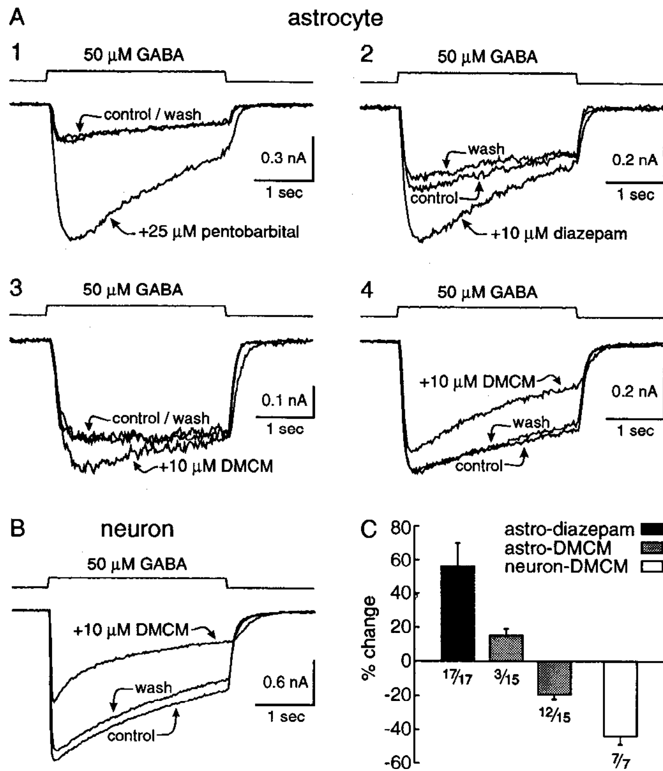

Figure 5. Modulation of the astrocytic GABA receptor by barbiturate and benzodiazepine receptor ligands. *A1,* A control inward current evoked by rapid application of 50 μM GABA. Coapplication of 50 μM GABA with 25 μM of the barbiturate sodium pentobarbital reversibly potentiated the GABA-evoked current. The whole-cell capacitance was 72 pF. *A2,* Control currents elicited by 50 μM GABA could be reversibly potentiated by coapplication of 10 μM diazepam, a benzodiazepine receptor modulator. The whole-cell capacitance was 65 pF. *A3,* In a subpopulation of astrocytes (20%), inward currents evoked by 50 μM GABA could be reversibly enhanced by coapplication of 10 μM DMCM, a benzodiazepine inverse agonist. The whole-cell capacitance was 65 pF. *A4,* In the remainder of astrocytes (80%), coapplication of 10 μM DMCM resulted in a depression of the GABA-activated current. The whole-cell capacitance was 56 pF. *B,* For comparison, reversible depression of a neuronal (CA1 pyramidal) inward current by DMCM is illustrated. The whole-cell capacitance was 16 pF. *C,* A summary of the benzodiazepine actions on GABA-activated currents from acutely isolated astrocytes (*astro*) and CA1 pyramidal neurons (*neurons*).

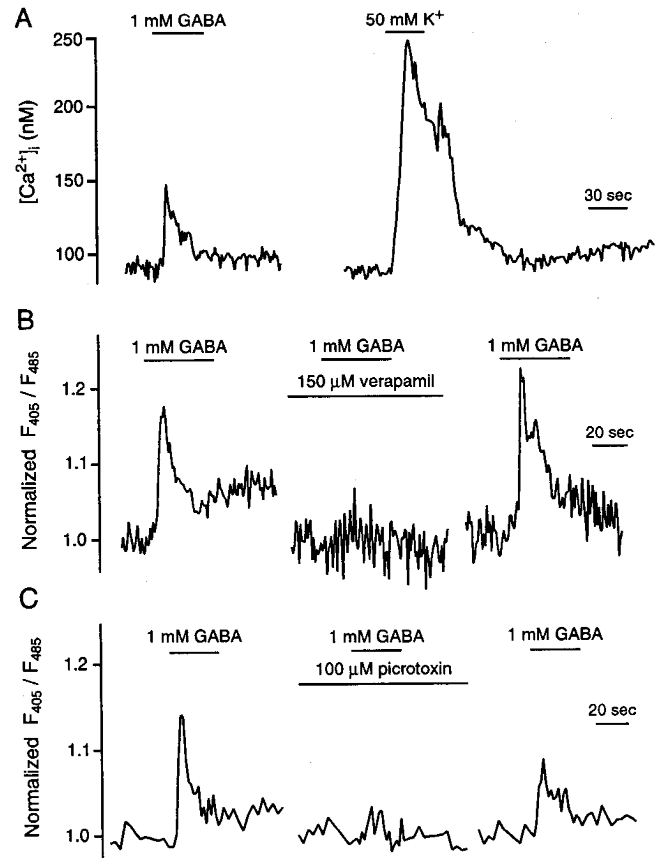

Figure 6. Activation of voltage-dependent Ca^{2+} channels in astrocytes by a GABA-evoked Cl^- efflux and subsequent depolarization. *A,* Superfusion of 1 mM GABA causes a transient increase in $[Ca^{2+}]_i$. For comparison, a transient increase in $[Ca^{2+}]_i$ evoked by superfusion of 50 mM K^+. *B,* For control, a transient increase in $[Ca^{2+}]_i$ was evoked by superfusion of 1 mM GABA. Coperfusion of 1 mM GABA and 150 μM verapamil, a Ca^{2+} channel blocker, reversibly depressed the GABA-evoked increase in $[Ca^{2+}]_i$. *C,* A transient increase in $[Ca^{2+}]_i$, evoked by superfusion of 1 mM GABA, was reversibly depressed by coperfusion of the Cl^- channel blocker picrotoxin (100 μM).

reversibly depressed the GABA-induced increase in $[Ca^{2+}]_i$ (*n* = 2; Fig. 6*C*).

Antibodies and Western blotting

Several antibodies were prepared that specifically recognized the $GABA_A$ receptor complex and its subunits at the immunoblot and immunocytochemical level (Gu et al., 1992, 1993; Perez-Velazquez and Angelides, 1993). Antibody 967 (PAb-967), generated against the affinity-purified $GABA_A$/benzodiazepine receptor of rat brain, recognized two closely spaced immunoreactive bands in the 52–56 kDa molecular mass range (Fig. 7*A*, lane 2). These bands corresponded to the predicted molecular mass for the population of $GABA_A$ receptor subunits (α, 48–53 kDa; β, 55–57 kDa) and the migration of these subunits in this 4–15% linear polyacrylamide gradient gel system. The immunodetection of the $GABA_A$ receptor subunits is specific since preimmune IgG from the same rabbit, 967, (Fig. 7*A*, lane 1) did not show any immunoreactivity. PAb-967 also did not show any immunoreactivity toward proteins extracted from red blood cells (data not shown), indicating that the recognitions of polypeptides in brain extracts was specific and represented the different components of the $GABA_A$ receptor. In addition, PAb-967 specifically recognized $GABA_A$ receptors in hippocampal cells in culture and in slices (data not shown) in a pattern that overlaid that of fluorescent benzodiazepine staining (Velazquez et al., 1989). PAb-967, however, did not immunoprecipitate ^{3}H-flunitrazepam binding sites from solubilized brain membranes.

Peptides corresponding to several regions of the $GABA_A$ receptor were synthesized as antigens in order to prepare sequence- and subunit-specific antibodies. Of the four that were injected, only two of the anti-peptide antibodies were positive in dot blots and Western blotting. These anti-peptide antibodies, generated against the α_1 subunit C-terminus (PAb-B) and β_1 subunit N-terminus (PAb-Q) of the $GABA_A$ receptor, recognized polypeptides at apparent molecular masses of 50 kDa (Fig. 7*B*, lane 2, *C,* lane 3) and 55 kDa (Fig. 7*B*, lane 4, *C,* lane 5), respectively. These molecular masses corresponded precisely to those predicted from the amino acid sequence encoded in the cDNA of these subunits in rat brain. The specificity of the recognition is shown by the absence of immunoreactivity of the

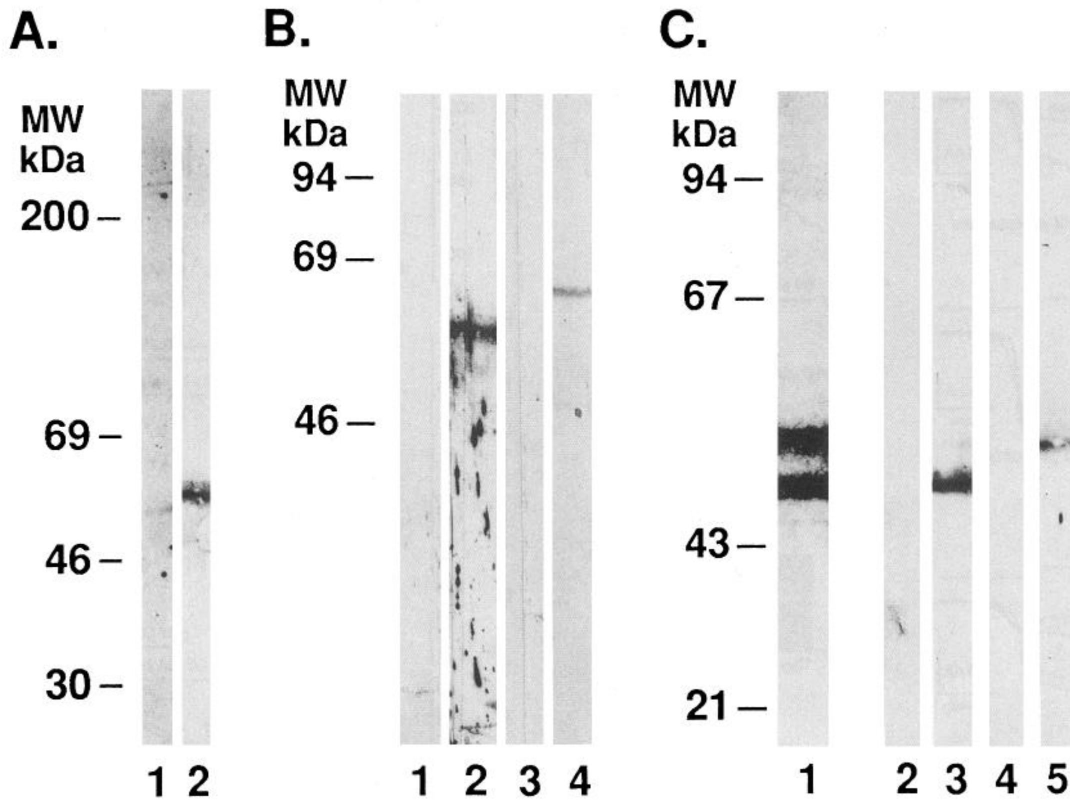

Figure 7. Immunoblots of three primary antibodies and their preimmune sera to purified $GABA_A$ receptors and crude glycoproteins from rat brain. *A,* Immunoblots with a polyclonal antibody generated against $GABA_A$/benzodiazepine receptors (PAb-967). A 4–15% linear polyacrylamide gel was loaded with 5–10 μg of benzodiazepine affinity-purified $GABA_A$ receptor from rat brain. *Lane 1,* Preimmune IgG; *lane 2,* immune IgG fraction. Dilutions of the antibodies were 1:50. *B,* Immunoblots with antibodies generated against either α_1 (PAb-B) or β_1 (PAb-Q) subunit peptides of the $GABA_A$ receptor. A 7.5% polyacrylamide gel was loaded with 10–20 μg of a crude glycoprotein preparation from rat brain. The ^{3}H-flunitrazepam-specific binding of the WGA eluent was 6.2 pmol/mg protein. *Lanes 1, 2,* Preimmune and immune serum for the antibody generated against the C-terminal peptide of the α_1 subunit. *Lanes 3, 4,* Preimmune and immune serum for the antibody generated against the N-terminal peptide of the β_1 subunit. Dilutions of the antisera were 1:50. *C,* Immunoblots with antibodies directed against either α_1 or β_1 subunit peptides of the $GABA_A$ receptor. A 7.5% polyacrylamide gel was loaded with 5–10 μg of benzodiazepine affinity-purified $GABA_A$ receptor from rat brain. Specific ^{3}H-flunitrazepam binding was 70 ± 10 pmol/mg protein. *Lane 1,* Silver-stained gel loaded with the purified $GABA_A$ receptor. *Lanes 2, 3,* Preimmune and immune IgG fractions for the antibody generated against the C-terminal peptide of the α_1 subunit. *Lanes 4, 5,* Preimmune and immune IgG fractions for the antibody generated against the N-terminal peptide of the β_1 subunit. Dilutions of the IgG fractions were 1:50.

preimmune IgG from each of the antibodies used (Fig. 7*B,* lanes 1, 3; *C,* lanes 2, 4). Further studies with the anti-peptide antibodies showed that, while they were not able to immunoprecipitate $GABA_A$ receptors from solubilized rat brain membranes, immunoblot and immunocytochemical analysis of both α_1- and β_1-transfected cells showed specific and high-affinity staining (Perez-Velazquez and Angelides, 1993). It is unlikely that PAb-B recognized additional α subunit isoforms (e.g., α_{2-6}) since the peptide sequence was entirely specific for the α_1 variant. It is possible that PAb-Q may have cross-reacted with the β_2 and β_3 variants, considering the degree of homology between the N-termini of the β subunits (Ymer et al., 1989), although we have no evidence for such cross-reactivity.

Immunocytochemical evidence for $GABA_A$ receptor expression

The expression and localization of $GABA_A$ receptors was determined by dual labeling acutely isolated astrocytes with a monoclonal antibody against GFAP (MAb-GFAP) and one of three polyclonal antibodies which recognize the $GABA_A$/benzodiazepine receptor (PAb-967), an α_1 subunit peptide (PAb-B), or a β_1 subunit peptide (PAb-Q). PAb-967, which recognizes multiple $GABA_A$ subunit isoforms, localized immunoreactivity on the astrocytic cell body and most large processes (Fig. 8*A*). In contrast, antibodies generated against either an α_1 subunit peptide (PAb-B; Fig. 8*B*) or a β_1 subunit peptide (PAb-Q; Fig. 8*C*) localized immunoreactivity predominantly on a distinct subset of processes. Pyramidal and fusiform neurons coisolated with astrocytes displayed intense labeling along the plasma membrane of both the soma and proximal dendrites (data not shown). The intensity of fluorescence was considerably greater for neurons than astrocytes. Control experiments in which the cells were incubated with preimmune sera did not display immunoreactivity (Fig. 8*D*). In addition, the immunoreactive product on astrocytes was similar whether the MAb-GFAP was present or omitted, suggesting that cross-reactivity between primary antibodies did not underlay the staining patterns.

Benzodiazepine binding on live astrocytes

The distribution of central $GABA_A$/benzodiazepine receptors on live astrocytes was determined by applying 5 nM of the fluorescent benzodiazepine derivative Ro 7-1986-BODIPY (Velazquez et al., 1989; McCabe et al., 1990). Total binding, revealed by laser-scanning confocal microscopy, was distributed in discrete clusters on both the cell body and a subset of processes (n =

11/11; Fig. 9*B*). Competitive displacement of specific binding by coperfusion of 500 nM diazepam revealed nonspecific binding (Fig. 9*C*). The average pixel intensity decreased by 77 ± 3% (range 64–88%, $n = 11$). In agreement with previous findings, specific binding on neurons was greatest on the soma with the fluorescence intensity tapering toward distal dendrites (data not shown; Velazquez et al., 1989). The pixel intensity on neurons was typically twofold greater than astrocytes, indicating higher benzodiazepine receptor density. Control experiments with either plasma membrane (DiI, $n = 3$; Nile red, $n = 2$) or lectin (concanavalin-A-tetramethylrhodamine; $n = 3$) markers revealed homogeneous fluorescence across the entire astrocytic membrane, indicating that fluorescent benzodiazepine hot spots were not due to excessive membrane folding or glycoprotein aggregation, respectively (data not shown; Velazquez et al., 1989). At the completion of experiments, a subpopulation of cells was fixed and immunostained for GFAP to verify its astrocytic phenotype ($n = 5/5$; Fig. 9*D*).

Discussion

The results of this study demonstrate that noncultured astrocytes from the mature rat hippocampus express abundant $GABA_A$ receptors. Analysis of benzodiazepine pharmacology indicates that astrocytic $GABA_A$ receptors are both heterogeneous among the astrocyte population and distinct from neuronal receptors. Activation of $GABA_A$ receptors in astrocytes results in an efflux of Cl^- which can significantly depolarize these cells to a potential at which voltage-gated Ca^{2+} channels open. Moreover, the data show that astrocytes, like neurons, target $GABA_A$ receptors and subunits to distinct cellular locations.

Electrophysiology

The GABA-activated Cl^- channel in cultured astrocytes has been shown to be similar to the neuronal $GABA_A$ channel (Blankenfeld and Kettenmann, 1992; Fraser et al., 1994). The present work indicates that acutely isolated astrocytes also have a GABA receptor coupled to a Cl^- channel. The GABA-activated Cl^- current was depressed by the $GABA_A$ receptor antagonist bicuculline and mimicked by muscimol, a selective $GABA_A$ receptor agonist. Moreover, the current had a reversal potential close to the Cl^- equilibrium potential and was depressed by the Cl^- channel blocker picrotoxin.

The astrocytic current evoked with a saturating concentration of GABA (1 mM) was one-half the amplitude of the current recorded under identical conditions in neurons. The whole-cell capacitance of astrocytes was typically fivefold larger than neurons, suggesting that average receptor density on neurons is considerably greater than on astrocytes. Nonetheless, $GABA_A$ receptor activation on astrocytes *in vivo* could evoke a substantial Cl^- efflux and localized membrane depolarization, since it is likely that the true current amplitude was underestimated. For example, the complex morphology of astrocytes and uneven distribution of receptors along the membrane undoubtedly compromised space-clamp control. In addition, enzymatic treatment with papain has been reported to abolish inhibitory postsynaptic potentials, suggesting proteolytic digestion of the receptor/channel complex (McCarren and Alger, 1987).

Recombinant studies have revealed that α subunit expression controls GABA receptor sensitivity (Levitan et al., 1988). Dose–response analysis of acutely isolated cells demonstrated that the ED_{50} was different between CA1 pyramidal neurons and astrocytes. The ED_{50} for pyramidal neurons (14 μM) was similar to recombinant receptors containing the α_1 subunit, whereas the ED_{50} for astrocytes (50 μM) is compatible with α_3 expression (Levitan et al., 1988). Caution must be exercised in interpretation of these results, however, since the whole-cell current is probably derived from multiple subunit combinations. Indeed, α_1 immunoreactivity on astrocytic processes was demonstrated in this study.

Functional expression of cloned subunits in combination with electrophysiological assays has demonstrated that the αβ subunit combination is sufficient for modulation by barbiturates (Schofield et al., 1987). Benzodiazepine modulation, however, requires the addition of a third subunit from the γ subfamily (Pritchett et al., 1989). In acutely isolated astrocytes, the GABA-activated inward current was modulated by barbiturate and benzodiazepine receptor ligands. Pentobarbital and diazepam potentiated the GABA-induced whole-cell current. These data are consistent with previous reports for cultured astrocytes (Bormann and Kettenmann, 1988; Rosewater and Sontheimer, 1994), cultured oligodendrocytes (Blankenfeld et al., 1991), and both cultured and acutely isolated neurons (e.g., Ransom and Barker, 1976; Kaneda et al., 1989; Twyman et al., 1989; Yakushiji et al., 1989). Both compounds increase the mean channel open time: barbiturates by increasing open duration and diazepam by increasing the frequency of opening (Twyman et al., 1989).

The benzodiazepine inverse agonist DMCM is known to depress the GABA-activated current in oligodendrocytes (Blankenfeld et al., 1991), neurons (Bormann et al., 1985; Puia et al., 1989; Bovolin et al., 1992), chromaffin cells (Bormann and Kettenmann, 1988), and a subpopulation of cultured astrocytes obtained from spinal cord ("fibrous"; Rosewater and Sontheimer, 1993). The compound decreased channel opening frequency, without altering conductance or opening duration (Vicini et al., 1987). In contrast, DMCM enhances the GABA-activated current in cultured astrocytes obtained from cortex (Backus et al., 1988; Bormann and Kettenmann, 1988), cerebellum (Bovolin et al., 1992), and spinal cord ("protoplasmic"; Rosewater and Sontheimer, 1993). Indeed, cultured astrocytes from cerebellum express high levels of the γ_1 subunit (Bovolin et al., 1992) which has been associated with DMCM enhancement of GABA-activated currents in recombinant studies (Puia et al., 1991). In 20% of acutely isolated astrocytes, DMCM also enhanced the GABA-activated current, suggesting that these $GABA_A$ receptors express similar subunit combinations. In the remaining 80% of astrocytes DMCM depressed the GABA responses, suggesting that an alternative γ subunit isoform was expressed. Interestingly, the DMCM-induced depression in astrocytes was less than one-half the depression observed in pyramidal neurons. The differential benzodiazepine pharmacology suggests subunit heterogeneity between not only astrocytes and neurons, but also within the astrocytic population.

GABA-activated Ca^{2+} influx

The increase in $[Ca^{2+}]_i$ induced by GABA could potentially occur through two mechanisms: influx through voltage-gated Ca^{2+} channels (MacVicar, 1984) and/or release from intracellular stores (Nilsson et al., 1993). Our finding that the GABA-activated increase in $[Ca^{2+}]_i$ was inhibited in the presence of either the Ca^{2+} channel blocker verapamil or the Cl^- channel blocker picrotoxin points to the former explanation. Verapamil did not diminish the GABA-activated current recorded in whole-cell mode; moreover, the presence of verapamil-sensitive Ca^{2+} channels has been demonstrated previously (Duffy and MacVicar,

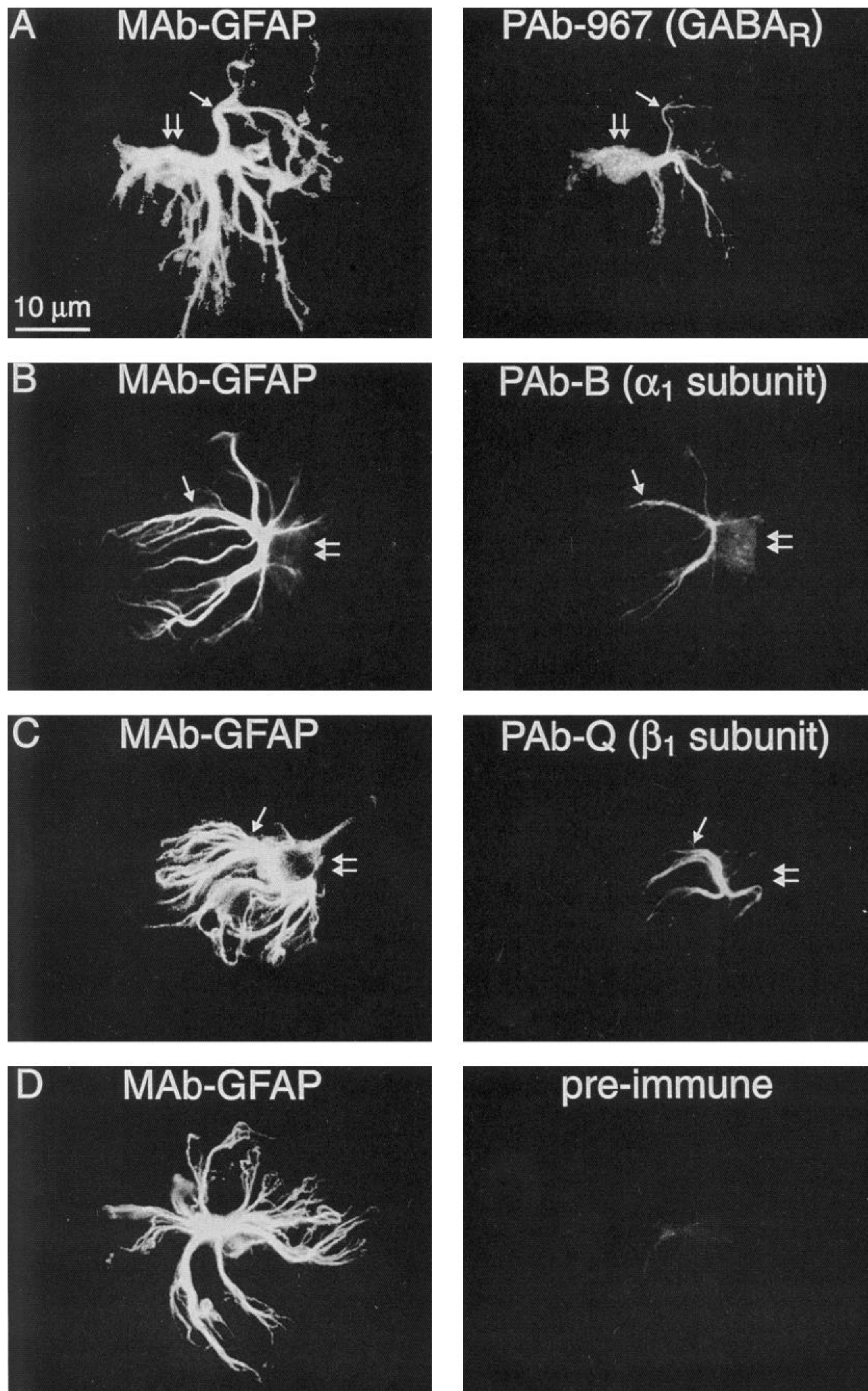

Figure 8. Digital micrographs of acutely isolated hippocampal astrocytes illustrating dual labeling for glial fibrillary acidic protein (MAb-GFAP) and either $GABA_A$/benzodiazepine receptors ($GABA_R$) or individual subunit peptides (α_1 or β_1). *A*, GFAP-positive astrocytes react with antisera

1994). The Ca^{2+} influx, therefore, was mediated by $GABA_A$-induced membrane depolarization.

The indo-1 experiments provide clues as to the magnitude and polarity of the membrane potential response to GABA. This could not be determined under whole-cell voltage clamp since the cell interior is dialyzed and the Cl^- gradient artificially distorted. The threshold for activating Ca^{2+} influx in acutely isolated astrocytes is reached when external K^+ is increased to 20 mM corresponding to a depolarization of approximately −45 mV (Duffy and MacVicar, 1994). These data indicate that GABA must depolarize the cell membrane to at least this potential, supporting previous studies suggesting that the Cl^- reversal potential in astrocytes is positive to resting potential (Kimelberg and Frangakis, 1985; Kettenmann et al., 1987).

Astrocytes *in vivo* are coupled extensively by gap junctions (Ransom and Carlini, 1986) and maintain a significant K^+ permeability at the resting membrane potential (Walz, 1989). Whether local depolarization by GABA could attain the activation threshold for Ca^{2+} channel opening *in vivo* is speculative, but may occur under certain conditions. For example, a constriction in the diameter of a process and clustering of the $GABA_A$ receptor/ionophore in close association with Ca^{2+} channels would facilitate local depolarization and Ca^{2+} channel activation. Furthermore, conditions which alter membrane and gap junction resistance (e.g., neurotransmitter modulation) could facilitate this event.

Subcellular localization of $GABA_A$ receptors

Until recently, immunocytochemical studies have generally failed to identify $GABA_A$ receptor expression in astrocytes (reviewed by Fraser et al., 1994). This lack of evidence may be due to lower levels of receptor expression making detection in tissue sections difficult. Indeed, the absolute amount of $GABA_A$ subunit mRNA expressed by astrocytes was two orders of magnitude less than neurons when quantified by competitive polymerase chain reaction (Bovolin et al., 1992). A lower expression of receptors is also consistent with our electrophysiological and anatomical assays. The antibody staining reported here is probably due to the increased resolution available with isolated cells in combination with the antigens chosen for antibody production (Gu et al., 1992, 1993; Perez-Velazquez and Angelides, 1993). Our data suggests that at least some astrocytic receptors may include the $\alpha_1\beta_1$ subunit combination, together with an unknown isoform of the γ subunit.

The specificity of the antibody staining in this study can be inferred by several observations: (1) purified receptors or subunit-specific peptide sequences were used as antigens; (2) selective recognition of subunit(s) from either crude glycoproteins or purified $GABA_A$ receptors on Western blots; (3) good correlation between immunoreactive patterns and fluorescence binding assays; (4) good correlation between neuronal staining and previously reported patterns; and (5) lack of staining with preimmune sera.

The immunoreactive patterns observed within hippocampal astrocytes suggests single-cell heterogeneity. Polyclonal antibody 967, which recognizes several subunits and possibly their isoforms, localized receptors to the cell body and a subset of processes. Cytoplasmic staining was observed, in agreement with previous immunocytochemical studies on astrocytes (Gu et al., 1993; Rosier et al., 1993), which may reflect receptor transport and/or turnover (Somogyi et al., 1989; Zimprich et al., 1991; Thompson et al., 1992). Polyclonal antibodies generated against either α_1 or β_1 subunit peptides revealed localization predominantly on astrocytic processes. Taken together, these data suggest $GABA_A$ subunits may be distributed differentially within single astrocytes. Perhaps the α_3 subunit, whose expression is suggested by our electrophysiological data, may be localized on the cell body which is typically devoid of α_1 subunit immunoreactivity. The $GABA_A$ receptors on the cell body may contain a β subunit other that the β_1 isoform (e.g., β_{2-4}), since PAb-967 and PAb-Q have been reported previously to recognize different subunits (Gu et al., 1993), or, alternatively, simply may not contain a β subunit (Fritschy et al., 1992). Interestingly, a monoclonal antibody generated against a similar portion of the β_1 subunit N-terminus resulted in similar staining of cerebral astrocytes that was distinct from the β_2 and β_3 isoform distribution (Rosier et al., 1993). A nonrandom distribution of subunits has been reported recently for neurons (Fritschy et al., 1992). Given the number of subunits identified, many combinations are possible which form a functional receptor. Recent evidence, however, would suggest that subunits assemble into preferred combinations (Angelloti et al., 1993). In fact, a single subunit combination may predominate in a particular cell (Fritschy et al., 1992) and subunit assembly may then determine cellular sorting (Perez-Velaquez and Angelides, 1993). In astrocytes, the α_1 and β_1 subunits may colocalize in a single receptor and thereby be targeted to distinct processes.

The benzodiazepine Ro 7-1986, which has high affinity and selectivity for central $GABA_A$ receptors (Gavish and Snyder, 1981), has been used previously for fluorescent ligand binding assays on membrane fractions and live cells (Valequez et al., 1989; McCabe et al., 1990). On live astrocytes, membrane-bound receptors were segregated into discrete patches on the cell body and distal processes. This observation is consistent with the immunoreactive findings and supported by previous studies on cultured astrocytes indicating an uneven distribution of $GABA_A$ receptors along the plasma membrane (Bormann and Kettenmann, 1988; Ventimiglia et al., 1990). $GABA_A$ receptors clustered on astrocytic processes may be in close proximity to inhibitory synapses, as has been recently demonstrated for Bergmann glial cells (Müller et al., 1994). Surprisingly, a high density of receptors are localized on the cell body. These receptors may be activated by neuronally released GABA, flowing out of the synaptic cleft, or alternatively by GABA release from adjacent astrocytes (Sarthy, 1985).

←

raised against $GABA_A$ receptors affinity purified on a benzodiazepine column (PAb-967). Note the punctate staining on the cell body (*double arrow*) and on numerous larger processes (*single arrow*). *B*, GFAP-positive astrocytes react with antisera generated against the α_1 subunit C-terminal peptide (PAb-B). Note that the staining is pronounced in a select subset of processes (*single arrow*). The cell body, marked by the *double arrow*, had weak levels of immunoreactivity. *C*, GFAP-positive astrocytes react with antisera generated against the β_1 subunit N-terminal peptide (PAb-Q). Note that the staining is pronounced in a select subset of processes (*single arrow*). The cell body, marked by the *double arrow*, was devoid of immunoreactivity. *D*, Staining was not observed on GFAP-positive astrocytes following substitution of the PAbs with their respective preimmune sera. In this example, PAb-967 was substituted with preimmune from rabbit-967.

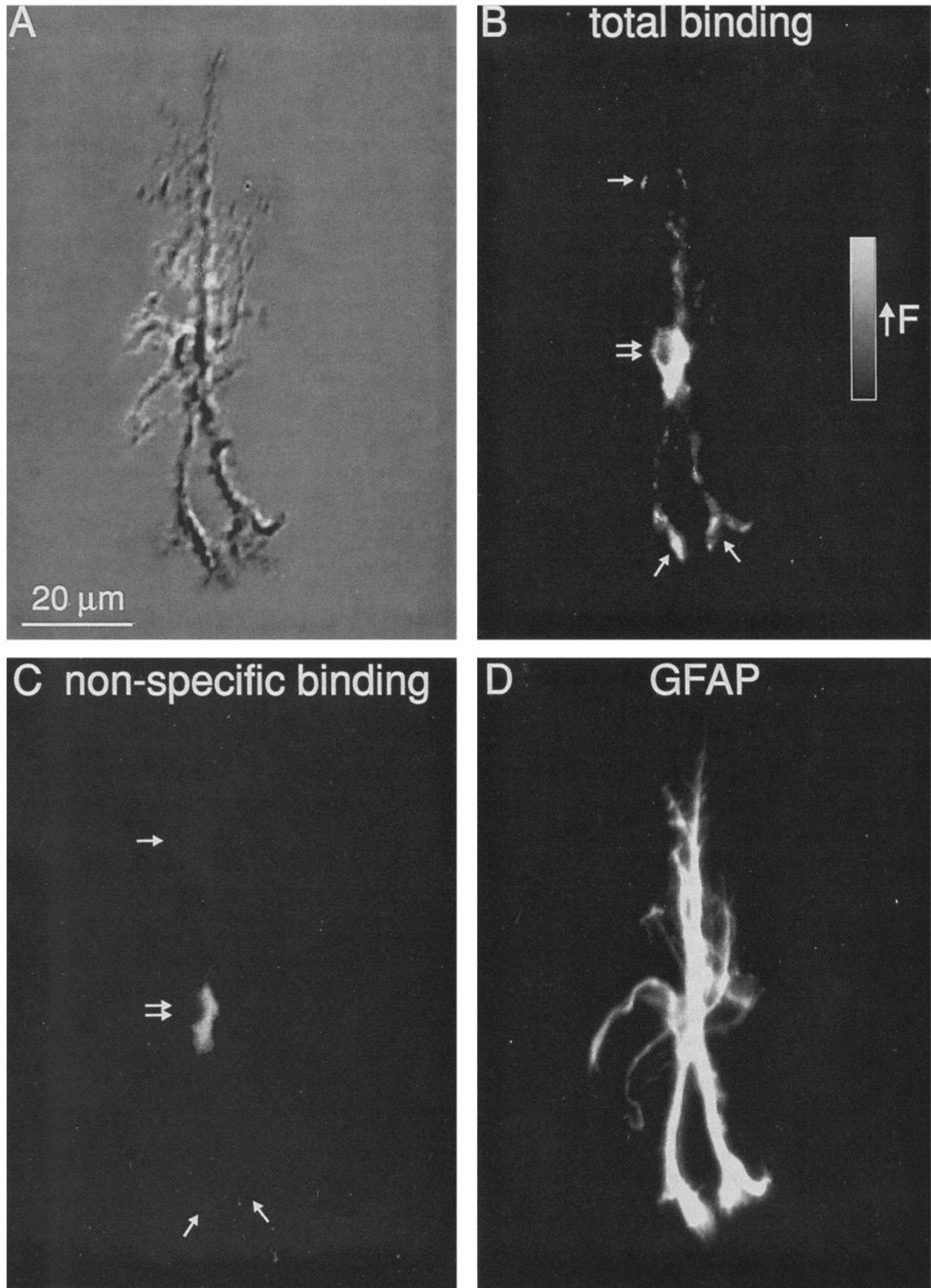

Figure 9. Subcellular localization of central benzodiazepine receptors on an acutely isolated astrocyte by use of a fluorescent benzodiazepine derivative. *A*, A digital photomicrograph of an acutely isolated hippocampal astrocyte. *B*, Areas of intense fluorescence indicate the subcellular expression of $GABA_A$/benzodiazepine receptors. The receptors are located on both the cell body (*double arrow*) and on several larger processes (*single arrows*). The black/white scale bar represents increasing fluorescence intensity (↑F). Fluorescent localization of benzodiazepine receptors was determined following a 20 min incubation in 5 nM of the derivative. *C*, Nonspecific binding was determined following coperfusion of 500 nM

Consequence of GABA receptor activation in the astrocytes

The physiological significance of astrocytic $GABA_A$ receptor activation remains speculative; however, $[Cl^-]_o$ and $[pH]_o$ homeostasis have been suggested (reviewed by Fraser et al., 1994). For example, a GABA-evoked Cl^- efflux from astrocytes could buffer $[Cl^-]_o$ in the vicinity of GABAergic synapses (Bormann and Kettenmann, 1988; MacVicar et al., 1989). The $GABA_A$ receptor/ionophore is also permeable to HCO_3^- ions (Bormann, 1988) which may underlie the extracellular alkalinization observed during inhibitory activity (Chesler and Chen, 1991; Kaila et al., 1991, 1992). Extracellular alkalinization augments presynaptic Ca^{2+} channels and thereby enhances neurotransmitter release (Barnes et al., 1993). In addition, elevations in $[HCO_3^-]_o$ could augment $[Cl^-]_o$ further by provoking anion exchange (Grover et al., 1993). Efflux of either anion could initiate Ca^{2+} influx via membrane depolarization and voltage-gated channels. As a consequence, astrocytes could respond to a GABA-induced elevation in $[Ca^{2+}]_i$ by a change in morphology (filopodia extension; Cornell-Bell and Finkbeiner, 1991) or their metabolic (glycogenolysis; Ververken et al., 1982) and functional (GABA transport; Sarthy, 1983) states. The combination of GABA receptors and Ca^{2+} channels, therefore, provide the appropriate tools for astrocytes to detect and respond to inhibitory neuronal activity.

References

Alvarez-Leemans FJ, Russel J (1990) Chloride channels and carriers in nerve, muscle and glial cells. New York: Plenum.

Angelotti TP, Uhler MD, Macdonald RL (1993) Assembly of $GABA_A$ receptor subunits: analysis of transient single-cell expression utilizing a fluorescent substrate/marker gene technique. J Neurosci 13:1418–1428.

Backus KH, Kettenmann H, Schachner M (1988) Effect of benzodiazepines and pentobarbital on the GABA-induced depolarization in cultured astrocytes. Glia 1:132–140.

Barnes S, Merchant V, Mahmud F (1993) Modulation of transmission gain by protons at the photoreceptor output synapse. Proc Natl Acad Sci USA 90:10081–10085.

Barres BA, Chun LLY, Corey DP (1989) Calcium current in cortical astrocytes: induction by cAMP, neurotransmitters, and permissive effect of serum factors. J Neurosci 9:3169–3175.

Berger T, Walz W, Schnitzer J, Kettenmann H (1992) GABA- and glutamate-activated currents in glial cells of the mouse corpus callosum slice. J Neurosci Res 31:21–27.

Blankenfeld G, Kettenmann H (1992) Glutamate and GABA receptors in vertebrate glial cells. Mol Neurobiol 5:31–43.

Blankenfeld G, Trotter J, Kettenmann H (1991) Expression and developmental regulation of a $GABA_A$ receptor in cultured murine cells of the oligodendrocyte lineage. Eur J Neurosci 3:310–316.

Bormann J (1988) Electrophysiology of $GABA_A$ and $GABA_B$ receptor subtypes. Trends Neurosci 11:112–116.

Bormann J, Clapham DE (1985) γ-aminobutyric acid receptor channels in adrenal chromaffin cells: a patch-clamp study. Proc Natl Acad Sci USA 82:2168–2172.

Bormann J, Kettenmann H (1988) Patch clamp study of GABA receptor Cl^- channels in cultured astrocytes. Proc Natl Acad Sci USA 85: 9336–9340.

Bormann J, Ferrero P, Guidotti A, Costa E (1985) Neuropeptide modulation of GABA-receptor Cl^- channels. Regul Pept [Suppl] 4:33–38.

Bovolin P, Santi MR, Puia G, Costa E, Grayson D (1992) Expression patterns of γ-aminobutyric acid type A receptor subunit mRNAs in primary cultures of granule neurons and astrocytes from neonatal rat cerebella. Proc Natl Acad Sci USA 89:9344–9348.

Burt DR, Kamatchi GL (1991) $GABA_A$ receptor subtypes: from pharmacology to molecular biology. FASEB J 5:2916–2923.

Chesler M, Chen JCT (1991) Alkaline extracellular pH shifts generated by two transmitter dependent mechanisms. Can J Physiol Pharmacol 70:S286–S292.

Chow TP, DeGrado WF, Knight E (1984) Antibodies to synthetic peptides of human interferon B. J Biol Chem 259:12220–12225.

Clark B, Mobbs P (1992) Transmitter-operated channels in rabbit retinal astrocytes studied *in situ* by whole-cell patch clamping. J Neurosci 6:2857–2863.

Cornell-Bell AH, Finkbeiner SM (1991) Ca^{2+} waves in astrocytes. Cell Calcium 12:185–204.

Duffy S, MacVicar BA (1994) Potassium-evoked Ca^{2+} influx in acutely isolated hippocampal astrocytes. Neuroscience 61:51–61.

Fraser DD, MacVicar BA (1991) Low-threshold transient calcium current in rat hippocampal lacunosum-moleculare interneurons: kinetics and modulation by neurotransmitters. J Neurosci 11:2812–2820.

Fraser DD, Duffy S, Hoppe D, Kettenmann H, MacVicar BA (1992) GABA-activated Cl^- current and Ca^{2+} influx in acutely isolated hippocampal astrocytes. Can J Physiol Pharmacol 70:Aix.

Fraser DD, Angelides KJ, MacVicar BA (1993) Subcellular localization of $GABA_A$ receptors on astrocytes using polyclonal antibodies and a fluorescent benzodiazepine derivative. Int Union Physiol Sci 32:244.30.

Fraser DD, Mudrick-Donnon LA, MacVicar BA (1994) Astrocytic GABA receptors. Glia 11:83–93.

Fritschy JM, Benke D, Mertens S, Oertel WH, Batchi T, Möhler H (1992) Five subtypes of type A γ-aminobutyric acid receptors identified in neurons by double and triple immunofluorescent staining with subunit-specific antibodies. Proc Natl Acad Sci USA 89:6726–6730.

Gavish M, Snyder SH (1981) γ-aminobutyric acid and benzodiazepine receptors: copurification and characterization. Proc Natl Acad Sci USA 78:1939–1942.

Gitman AG, Kahane I, Loyter A (1985) Use of virus-attached antibodies or insulin molecules to mediate fusion between sendai virus envelopes and neuraminidase-treated cells. Biochemistry 24:2762–2765.

Grover LM, Lambert NE, Schwartzkroin PA, Teyler TJ (1993) Role of HCO_3^- ions in depolarizing $GABA_A$ receptor-mediated responses in pyramidal cells of rat hippocampus. J Neurophysiol 69:1541–1555.

Grynkiewics G, Poenie M, Tsien RY (1985) A new generation of Ca^{2+} indicators with greatly improved fluorescence properties. J Biol Chem 260:3440–3450.

Gu Q, Velazquez JLP, Angelides KJ, Cynader MS (1992) $GABA_A$ receptor immunoreactivity in the white matter. Neuroreport 3:169–172.

Gu Q, Velazquez JLP, Angelides KJ, Cynader MS (1993) Immunocytochemical study of $GABA_A$ receptors in the cat visual cortex. J Comp Neurol 333:94–108.

Hoppe D, Kettenmann H (1989) GABA triggers a Cl^- efflux from cultured mouse oligodendrocytes. Neurosci Lett 97:334–339.

Kaila K, Panula P, Karhunen T, Heinonen E (1991) Fall in intracellular pH mediated by $GABA_A$ receptors in cultured rat astrocytes. Neurosci Lett 126:9–12.

Kaila K, Paalasmaa P, Taira T, Voipio J (1992) pH transients due to monosynaptic activation of $GABA_A$ receptors in rat hippocampal slices. Neuroreport 3:105–108.

Kaneda M, Wakamori M, Akaike N (1989) GABA-induced chloride current in rat isolated purkinje cells. Am J Physiol 256:C1153–1159.

Kay A, Wong RKS (1986) Isolation of neurons suitable for patch-clamping from adult mammalian central nervous system. J Neurosci Methods 16:227–238.

Kettenmann H (1990) Chloride channels and carriers in cultured glia cells. In: Chloride channels and carriers in nerve, muscle, and glial cells (Alvarez-Leefmans FJ, Russell JM, eds), pp 193–208. New York: Plenum.

←

diazepam with the fluorescent benzodiazepine derivative for 20 min. The majority of benzodiazepine receptor labeling was competitively displaced. The fluorescent image was obtained under identical optical conditions, as in *B. D,* At the completion of the experiment, the cell was fixed and immunostained for GFAP to verify its astrocytic phenotype.

Kettenmann H, Schachner M (1985) Pharmacological properties of GABA, glutamate and aspartate induced depolarizations in cultured astrocytes. J Neurosci 5:3295–3301.

Kettenmann H, Backus BH, Schachner M (1987) γ-aminobutyric acid opens Cl-channels in cultured astrocytes. Brain Res 404:1–9.

Kimelberg HK (1990) Chloride transport across glial membranes. In: Chloride channels and carriers in nerve, muscle, and glial cells (Alvarez-Leefmans FJ, Russell JM, eds), pp 159–191. New York: Plenum.

Kimelberg HK, Frangakis MV (1985) Furosemide- and bumetanide-sensitive ion transport and volume control in primary astrocyte cultures from rat brain. Brain Res 61:125–134.

Kirchhoff F, Kettenmann H (1992) GABA triggers a $[Ca^{2+}]_i$ increase in murine precursor cells of the oligodendrocyte lineage. Eur J Neurosci 4:1049–1058.

Laemmli K (1970) Cleavage of structural proteins during the assembly of the head of bacteriophage T4. Nature 277:680–685.

Levitan ES, Schofield PR, Burt DR, Rhee LM, Wisden W, Kohler M, Fujita N, Rodriguez N, Stephenson FA, Darlison MG, Barnard EA, Seeburg PH (1988) Structural and functional basis for $GABA_A$ receptor heterogeneity. Nature 335:76–79.

MacVicar BA (1984) Voltage-dependent Ca^{2+} channels in glial cells. Science 226:1345–1347.

MacVicar BA, Tse FWY (1988) Norepinephrine and cyclic adenosine 3′:5′-cyclic monophosphate enhances a nifedipine-sensitive calcium current in cultured rat astrocytes. Glia 1:359–365.

MacVicar BA, Tse FWY, Crichton SW, Kettenmann H (1989) GABA-activated Cl^- channels in astrocytes of hippocampal slices. J Neurosci 9:3577–3583.

MacVicar BA, Fraser DD, Duffy S (1992) Preparation of astrocytes: primary cell culture and acute isolation. In: Practical electrophysiological methods (Kettenman H, Grantyn R, eds), pp 101–104. New York: Wiley-Liss.

McCabe RT, De Costa BR, Miller RL, Havunjian RH, Rice KC, Skolnick P (1990) Characterization of benzodiazepine receptors with fluorescent ligands. FASEB J 4:2934–2940.

McCarren M, Alger B (1987) Papain effects on rat hippocampal neurons in the slice preparation. Neurosci Lett 78:307–310.

Mudrick-Donnon LA, Williams PJ, Pittmann QP, MacVicar BA (1993) Postsynaptic potentials mediated by GABA and dopamine evoked in stellate glial cells of the pituitary pars intermedia. J Neurosci 13: 4660–4666.

Müller T, Fritschy JM, Grosche J, Pratt GD, Möhler H, Kettenmann H (1994) Developmental regulation of voltage-gated K^+ channels and $GABA_A$ receptor expression in Bergmann glial cells. J Neurosci 14: 2503–2514.

Nilsson M, Eriksson PS, Rönnbäck L, Hansson E (1993) GABA induces Ca^{2+} transients in astrocytes. Neuroscience 54:605–614.

Olsen RW, Tobin AJ (1990) Molecular biology of $GABA_A$ receptors. FASEB J 4:1469–1480.

Perez-Velazquez JL, Angelides KJ (1993) Assembly of GABA receptor subunits determines cellular sorting and localization in neurons. Nature 361:457–460.

Peters A, Palay SL, Webster HD (1991) The fine structure of the nervous system. New York: Oxford UP.

Pritchett DB, Sontheimer H, Shivers BD, Ymer S, Kettenmann H, Schofield PR, Seeburg PH (1989) Importance of a novel $GABA_A$ receptor subunit for benzodiazepine pharmacology. Nature 338:582–585.

Puia G, Santi MR, Vicini S, Pritchett DB, Seeburg PH, Costa E (1989) Differences in the negative allosteric modulation of γ-aminobutyric acid receptors illicited by 4′-chlorodiazepam and by a β-carboline-3-carboxylate ester: a study with natural and reconstituted receptors. Proc Natl Acad Sci USA 86:7275–7279.

Puia G, Vicini S, Seeburg PH, Costa E (1991) Influence of recombinant γ-aminobutyric acid-A receptor subunit composition on the action of allosteric modulators of γ-aminobutyric acid-gated Cl^- currents. Mol Pharmacol 39:691–696.

Ransom BR, Barker JL (1976) Pentobarbital selectively enhances GABA-mediated post-synaptic inhibition in tissue cultured mouse spinal neurons. Brain Res 114:530–535.

Ransom BR, Carlini WG (1986) Electrophysiological properties of astrocytes. In: Astrocytes (Fedoroff S, Vernadakis A, eds), pp 1–49. Orlando: Academic.

Rosewater K, Sontheimer H (1994) Fibrous and protoplasmic astrocytes express $GABA_A$ receptors that differ in benzodiazepine pharmacology. Brain Res 636:73–80.

Rosier A, Arckens L, Orban GA, Vandesande F (1993) Immunocytochemical detection of astrocyte $GABA_A$ receptors in cat visual cortex. J Histochem Cytochem 41:685–692.

Sarthy PV (1983) Release of $[^3H]$γ-aminobutyric acid from glial (muller cells) of the rat retina: effects of K^+, veratridine and ethylenediamine. J Neurosci 3:2494–2503.

Schofield PR, Darlison MG, Fugita N, Burt DR, Stephenson FA, Rodriguez H, Rhee LM, Ramachandran J, Reale V, Glencorse TA, Seeburg PH, Barnard EA (1987) Sequence and functional expression of the $GABA_A$ receptor show a ligand-gated receptor superfamily. Nature 328:221–227.

Sigel W, Mamalaki C, Barnard EA (1982) Isolation of a GABA receptor from bovine brain using a benzodiazepine affinity column. FEBS Lett 147:45–48.

Somogyi P, Takagi H, Richards JG, Möhler H (1989) Subcellular localization of $GABA_A$/benzodiazepine receptors in the cerebellum of rat, cat and monkey using monoclonal antibodies. J Neurosci 9:2197–2209.

Steinhäuser C, Berger T, Frotscher M, Kettenmann H (1993) Voltage- and ligand-gated membrane current pattern of identifiable glial cells in the hippocampal slice. In: Slow activity changes in the brain (Haschke W, Speckmann EJ, eds), pp 179–190. Boston: Birkhäuser.

Steinhäuser C, Jabs R, Kettenmann H (1994) Properties of GABA and glutamate responses in identified glial cells of the mouse hippocampal slice. Hippocampus 4:19–36.

Thompson CL, Bodewitz G, Stephenson FA, Turner JD (1992) Mapping of $GABA_A$ receptors α_5 and α_6 subunit-like immunoreactivity in rat brain. Neurosci Lett 144:53–56.

Towbin H, Stahelin T, Gordon J (1979) Electrophoretic transfer of proteins from polyacrylamide gels to nitrocellulose sheets: procedure and some applications. Proc Natl Acad Sci USA 76:4350–4354.

Tse FWY, Fraser DD, Duffy S, MacVicar BA (1992) Voltage-activated K^+ channels in acutely isolated hippocampal astrocytes. J Neurosci 12:1781–1788.

Twyman RE, Rodgers CJ, Macdonald RL (1989) Differential regulation of γ-aminobutyric acid receptor channels by diazepam and phenobarbital. Ann Neurol 25:213–220.

Velazquez JLP, Thompson CL, Barnes EM Jr, Angelides KJ (1989) Distribution and lateral mobility of GABA/benzodiazepine receptors on nerve cells. J Neurosci 9:2163– 2169.

Ventimiglia R, Grierson JP, Gallombardo P, Sweetman PM, Tallman JF, Geller HM (1990) Cultured rat neurons and astrocytes express immunologically related epitopes of the $GABA_A$/benzodiazepine receptor. Neurosci Lett 115:131–136.

Ververken D, Van Veldhoven P, Proost C, Carton H, De Wulf H (1982) On the role of Ca^{2+} ions in the regulation of glycogenolysis in mouse brain cortical slices. J Neurochem 38:1286–1295.

Vicini S, Mienville JM, Costa E (1987) Actions of benzodiazepine and β-carboline derivatives on γ-aminobutyric acid Cl^- channels recorded from membrane patches of neonatal rat cortical neurons in culture. J Pharmacol Exp Ther 243:1195–1201.

Walz W (1989) Role of glia cells in the regulation of the brain ion microenvironment. Prog Neurobiol 33:309–333.

Yakushiji T, Tokutomi N, Akaike N (1989) Augmentation of GABA-induced chloride current in frog sensory neurons by diazepam. Neurosci Res 6:309–320.

Ymer S, Schofield PR, Draguhn A, Werner P, Köhler M, Seeburg PH (1989) $GABA_A$ receptor β subunit heterogeneity: functional expression of cloned cDNAs. EMBO J 8:1665–1670.

Zimprich F, Zezula J, Sieghart W, Lassmann H (1991) Immunohistochemical localization of the α_1, α_2 and α_3 subunit of the $GABA_A$ receptor in the rat brain. Neurosci Lett 127:125–128.